Design and analysis of double-gate junctionless vertical TFET for gas sensing applications

Sonal Singh[1] · Mamta Khosla[1] · Girish Wadhwa[1] · Balwinder Raj[1]

Abstract

In this present study, junctionless vertical tunnel field-effect transistor (JL-VTFET) with catalytic metals as gate contacts is proposed for gas sensing applications. The vertical double-sided gate architecture provides better gate controllability over conventional TFETs for band-to-band tunneling (BTBT). An architecture for n-channel JL-VTFET with Palladium (Pd) as gate metal is analyzed for Hydrogen sensing, while Cobalt (Co) and Molybdenum (Mo) metals as gate contacts are analyzed for Ammonia sensing. P + pockets are created near the source region by using work function values befitting the aforementioned catalytic metals. Characteristics of the proposed structure are studied considering the electric field, surface potential, and energy bandgap graphs concerning adsorption of gas molecules, using Silvaco ATLAS TCAD simulator. Simulation results of JL-VTFET with 50-nm gate length show good sensitivity calibrations ($S_{\text{Idoff}} \sim 1.99 \times 10^3$, 2.09×10^3 and 6.43×10^2) and high $I_{\text{don}}/I_{\text{doff}}$ ratio ($\sim 4.3 \times 10^9$, $\sim 2.01 \times 10^7$ and 1.33×10^{12}) for Co, Mo and Pd as gate metals, respectively

Keywords Vertical TFET · Junction-less · Gas sensor · Gate stack · BTBT

1 Introduction

The ever-evolving VLSI industry is exploring ultralow power consuming devices that fulfill nanoscale fabrication, high package density, high sensitivity and at the same time, are also technologically feasible. As we follow Moore's Law beyond the 20 nm regime, a fabricating highly doped junction pose serious issues like random dopant fluctuations (RDF) and requires costly techniques of ion implantation and diffusion. Junction less transistor, that does not involve fabrication of any junction, is a sublime option as a coming of age device. Scaling the device dimensionally also reduces the energy requirements manifolds. However, conventional field-effect transistors (FETs) need at least 60 mV to be applied at the gate terminals to upgrade the current by one order at room temperature. Tunnel FETs (TFET), with enhanced operations in switching speed, steeper subthreshold slope (< 60 mV/decade) and power efficiency [1], have emerged as a potential substitute for further diversification of Moore's concept. TFET based sensors have been explored on various fronts: (1) using suitable sensitive films based on catalytic metals, organic compounds, polymers, metal compounds and some hydrated salts [2–5]; and (2) device engineering [6–9] based on novel architecture [10–13], optimization [14–18] and doping technique variations [19, 20].

The essential theory behind TFET based sensors is the band-to-band (BTBT) tunneling mechanism, which controls carrier transport, to detect pernicious gaseous molecules in the surroundings. Over the last decade, various architectures have been exploited for ammonia gas sensing [21] by Fine, Wollenstein, Lopez et al. [22–24]. Bjorn timmer et al. [25] had put forth extensive research work on the advantages of detecting gaseous ammonia over solid-state ammonia. This is due to the fact that extremely low concentrations of any toxic material (~ 2 ppb) is easier to detect while dealing with gaseous state matter rather than solid. This study has been instrumental in designing environmental scanner and breathe analyzers for patients. Similar studies have been

✉ Girish Wadhwa
girishw.17.phd@nitj.ac.in

Sonal Singh
singhsonal9494@gmail.com

Mamta Khosla
khoslam@nitj.ac.in

Balwinder Raj
rajb@nitj.ac.in

1. Nanoelectronics Research Lab, Department of Electronics and Communication Engineering, NIT Jalandhar, Jalandhar, India

done regarding Hydrogen gas sensing by Tsukada [3], Gautam et al. [8]. However, vertical double-gate junctionless TFET structure has not been investigated for gas sensing applications. Blending the advantages of vertical architecture and gate stacking technique, a junction-less vertical tunnel field-effect-transistor (JL-VTFET) based gas detecting device has been realized using a heavily doped Silicon body $(1 \times 10^{19}$ cm$^{-3})$. Since no metallurgical junction is needed, the fabrication process is facile. Also, uniform concentrations in the tunneling direction yields improved electrical properties along with marginal variations. Absence of sharp doping gradients aide in lesser short channel effects for the device [16]. VTFETs are not bounded by channel length constraints, thus widening this innovation beyond 10 nm and the advantages of the less on-chip area. The ongoing aggressive device shrinking trend calls for shrinking of gate oxide thickness, utilizing effective oxide thickness of SiO$_2$ around 0.5 nm, stacked with HfO$_2$. With excellent thermal stability, high dielectric constant and lower bulk trap density, HfO$_2$ is a suitable alternative for low power nanoscale devices [9]. Excluding the doping concentration gradient factor leads to the absence of steep and irregular junctions connecting the drain, channel and source, which further facilitates the architecture of JL-VTFET over conventional TFETs.

2 Proposed design and device calibration

Figure 1 represents the two-dimensional schematics of the proposed JL-VTFET. The *x*-axis contours the width while the *y*-axis contours the length of the device. The conventional gate oxide is replaced by SiO$_2$/HfO$_2$ stacked gate oxide integrated bilaterally across the channel. For making the device junction less, n-type doping of 1×10^{19} cm^{-3} is used as a silicon body, with channel length (L_{ch}) of 50 nm and channel thickness (T_{ch}) of 10 nm. Platinum metal contacts with work function (ϕ_{ms}) of 5.93 eV have been used for source electrodes to create p$^+$ pockets. Highly reactive catalytic metals Cobalt ($\phi_M = 5.0$ eV) and Molybdenum ($\phi_M = 4.4$–4.95 eV) have been used as gate metal for ammonia gas [1] while Palladium ($\phi_M = 5.2$–5.5 eV) has been used for Hydrogen gas sensing [8] due to their high reactivity towards the respective gases. This validates the wide range of operation of the proposed structure. This negates the use of external doping requirements and thus deals with random dopant fluctuation (RDF) issues. The device is studied at a drain-to-source voltage (V_{ds}) and gate-to-source voltage (V_{gs}) of 1 V each. Concentration-mobility model (CONMOB) [14] for relating low field mobilities of charge carriers at room temperature, band-gap-narrowing model (BGN) [14] for examining bipolar heavily doped portions, band-to-band-nonlocal model (BBT.NONLOCAL) [14] for modeling tunneling currents and Shockey-Reed-Hall
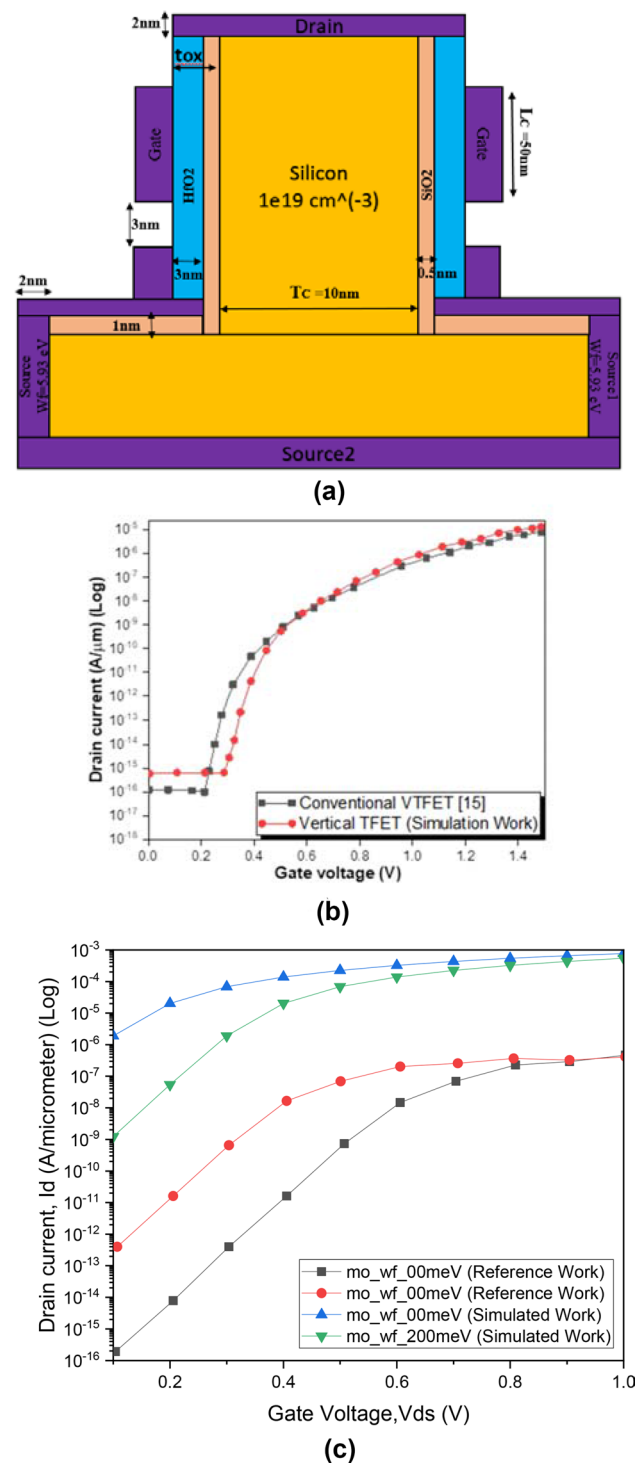
(a)

(b)

(c)

Fig. 1 a Two-dimensional cross-sectional view of junction less VTFET. **b** Simulated output characteristic of the junction less VTFET in contrast with the conventional device. **c** Comparison of the Transfer characteristics curve for Molybdenum as a catalytic gate electrode between simulated results and reference work [1]

Table 1 List of parameters used for the proposed JL-VTFET gas sensing device

Parameters	Symbol	Parameters
Length of channel	L_C	50 nm
Thickness of channel	T_C	10 nm
Doping	N_D	1×10^{19} cm^{-3}
Gate stack thickness SiO$_2$/HfO$_2$	t_{ox}	0.5 nm/3 nm
Source work function	ϕ_{ms}	5.93 eV
Drain bias	V_{ds}	1 V

Table 2 Sensitivity calculations of JL-VTFET based gas sensor using cobalt gate electrodes

$\Delta\phi_M$ (eV)	I_{doff} (A/μm)	I_{don} (A/μm)	I_{don}/I_{doff}	S_{Idoff}
Without gas	1.83e–10	6.01e–4	3.28e+06	–
50	2.71e–11	5.44e–4	2.01e+07	6.75e+00
100	4.02e–12	4.87e–4	1.21e+08	4.55e+01
150	5.93e–13	4.32e–4	0.73e+09	3.09e+02
200	8.75e–14	3.78e–4	0.43e+10	2.09e+03

Table 3 Sensitivity calculations of JL-VTFET based gas sensor using molybdenum gate electrodes

$\Delta\phi_M$ (eV)	I_{doff} (A/μm)	I_{don} (A/μm)	I_{don}/I_{doff}	S_{Idoff}
Without gas	5.41e–08	7.67e–4	1.42e+04	–
50	8.21e–09	7.13e–4	0.87e+05	6.59e+00
100	1.23e–09	6.57e–4	5.34e+05	4.39e+01
150	1.83e–10	6.01e–4	3.28e+06	2.96e+02
200	2.71e–11	5.44e–4	2.01e+07	1.99e+03

Table 4 Sensitivity calculations of JL-VTFET based gas sensor using palladium gate electrodes

$\Delta\phi_M$ (eV)	I_{doff} (A/μm)	I_{don} (A/μm)	I_{don}/I_{doff}	S_{Idoff}
Without gas	8.75e–14	3.78e–4	0.43e+10	–
50	1.30e–14	3.25e–4	2.51e+10	6.73e+00
100	2.04e–15	2.74e–4	1.34e+11	4.29e+01
150	4.14e–16	2.26e–4	0.55e+12	2.11e+02
200	1.36e–16	1.81e–4	1.33e+12	6.43e+02

recombination model (SRH) [14] for examining electron lifetime dependency on doping and temperature, have been deployed for studying the simulations of the proposed structure at nanoscale level. Table 1 enlists the structural parameters utilized here.

The reproduction boundaries and model properties for the two-dimensional junction less VTFET are taken like that of a traditional VTFET [15] with the exception of the utilization of a higher doping in the channel region. The proposed device is calibrated with the experimental data of VTFET [15] as appearing in Fig. 1b and the detailed information of the channel current is acquired with the assistance of the Plot Digitizer tool. All the simulations of vertical TFET have been done utilizing the Silvaco 2D-ATLAS tool.

2.1 Comparison between referenced structure and proposed vertical TFET structure

The vertical double-sided gate architecture provides better gate controllability over conventional structures for band-to-band tunneling (BTBT). The proposed device can be used for gas sensing applications because of its subthreshold slope or swing (S) and high I-ON current. Architecture for n-channel JL-VTFET with Molybdenum (Mo) metal as gate contacts is analyzed for Ammonia sensing. In Fig. 1c, the I-ON current is quite high as compared to the referenced structure. The sensitivity factors for JL-VTFET based sensor using Cobalt, Molybdenum, and Palladium as the gate metal electrodes are much better as compared to previous gas sensor structure (Sensitivity calculations are enlisted in Tables 2, 3, 4).

3 JL-VTFET working principle and characteristics

Gas sensors work on the principle of conversion of concentrations of various gaseous molecules into standard electrical signals by using specific physical and chemical effects. When gas molecules of harmful gases, like hydrogen and ammonia, react with catalytic metals' surface at the gate contacts, it brings in a change in the gate work function. Equation (1) represents work function variability on account of adsorption of pernicious gas molecules [22].

$$\Delta\phi_M = \text{cont} - \left[\left(\frac{RT}{4F} \right) \times \ln(P) \right] \qquad (1)$$

where R denotes the gas constant, T is the absolute temperature, F denotes Faraday's constant, and P denotes partial pressure of the gas. The relational dependency of the partial pressure of a gas on its concentrations can be utilized to calibrate the device in terms of mole fractions of the gas in the air. TFETs show $\sim 1.4 \times V_{th}$ standard deviation than conventional MOSFETs and most of their attributes are evaluated by work function values of gate metals near the source where band-to-band (BTBT) tunneling occurs [11]. Thus work function variations cause changes in threshold voltage (V_{th}) and flat band voltage (V_{fb}) which further alters the drain current (I_{don} and I_{doff}).

The dependency of V_{fb} on WFV is represented through Eq. (2) [8].

$$V_{fb} = \phi_M - \phi_S \pm \Delta\phi_M \tag{2}$$

where ϕ_M denotes the metal work function, $\Delta\phi_M$ denotes the gate-metal-work-function variation and ϕ_S denotes the work function of silicon given by Eq. (3) [8].

$$\phi_S = \frac{E_g}{2} + \chi - q\phi_{fp} \text{ for n - channel} \tag{3}$$

The variations in V_{th} affect the subthreshold current of the device, which changes the OFF current (I_{doff}) represented by Eq. (4) [1].

$$I_{subthreshold} = I_o\left[e^{\frac{V_{gs}-V_{th}}{\eta V_T}}\right]\left[1 - e^{\frac{-V_{ds}}{V_T}}\right] \tag{4}$$

where $I_o = \frac{w\mu_n C_{ox} V_T^2 e^{1.8}}{L} V_T$.

V_{gs}, V_{ds} and V_T are the gate-to-source, drain-to-source and thermal voltages of the device respectively. L and w denote the length and the effective width of the transistor respectively. Cox denotes the oxide capacitance of gate, η denotes the coefficient of subthreshold swing and μ_n denotes electron mobility. Hence, the above-mentioned equations set forth the relations between WFV, threshold voltage and currents of the transistor.

For studying the conduction actions of the proposed JL-VTFET, we go through the electric field, surface potential and energy band characteristic curves. Figure 2a shows that more the change in work function ($\Delta\phi_M$), greater is the electric field value attained due to decreased mobility of charge flow in the channel. The electric field is outlined as the gradient product of electron density of states and Fermi–Dirac distribution function. Figures 3, 4 describe the electric field and corresponding potential variation with respect to the various gate metal contacts respectively. In the drain region, there is a steady increase in electric field value which reflects as a constant, gently declining slope in the potential curve. As we move across the length of the device, electric field attains its maximum value across the channel.
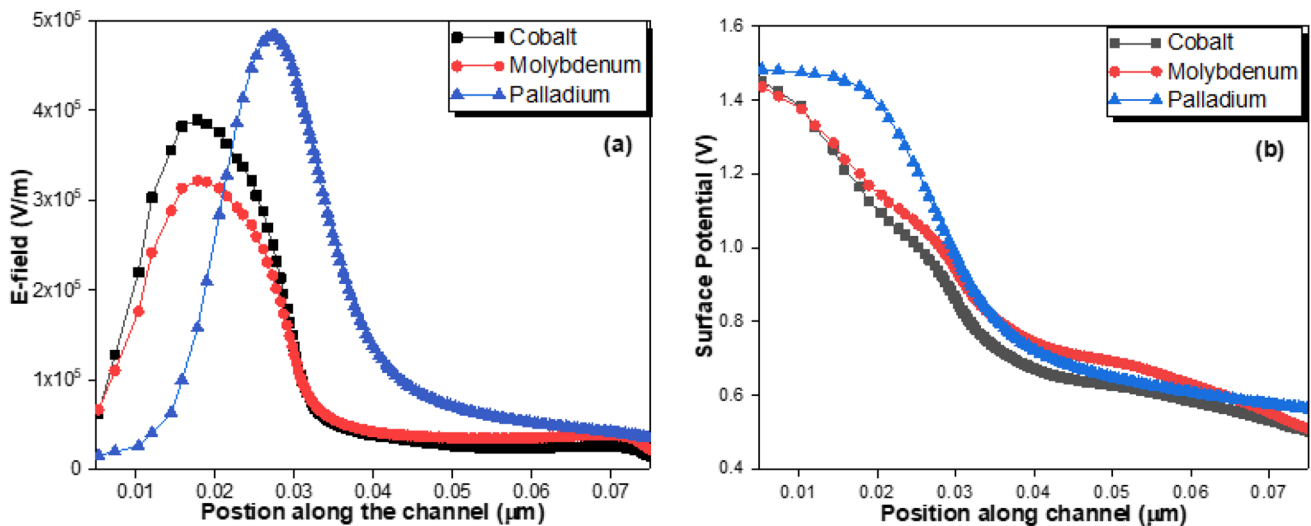

Fig. 2 Device characteristics plots of **a** Electric field, **b** Channel potential of JL-VTFET in ON state ($V_{ds} = 1$ V and $V_{gs} = 1$ V)
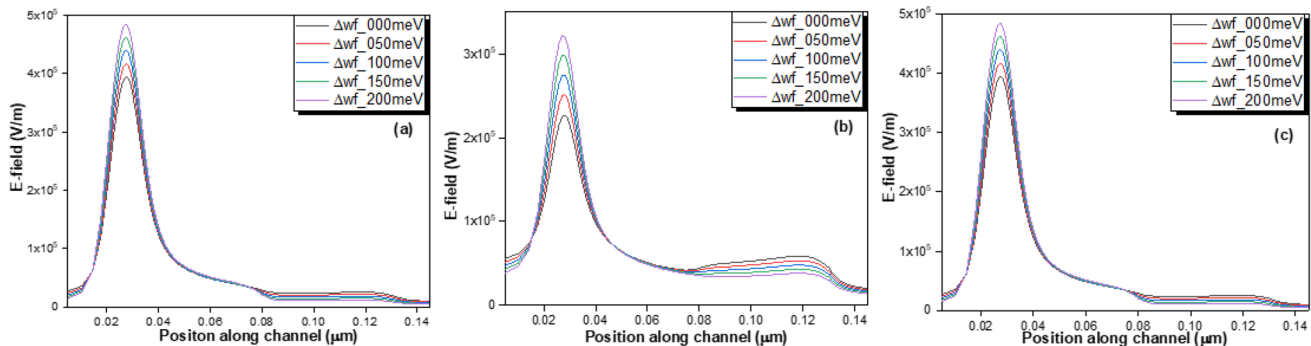

Fig. 3 Electric field plots along the channel for **a** Cobalt, **b** Molybdenum, and **c** Palladium w.r.t work function variations
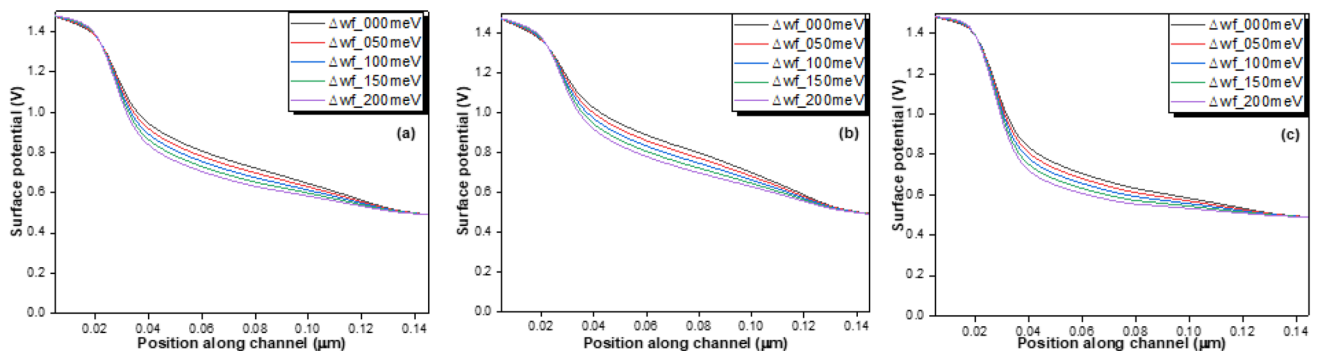
Fig. 4 Surface potential plots along the channel for **a** Cobalt, **b** Molybdenum, and **c** Palladium w.r.t work function variations

A dip starts shortly after this due to decrease in energy of the device. The channel region experiences a sharp decline in an electric field, followed by an almost constant slope. A slight increase near the tunneling area is observed in the source region near the channel, followed by a constant slope. Considering potential as the negative integral of an electric field [1], a reversal in the graph can be seen in the drain and channel regions.

Figure 5 describes a shift in the energy band diagrams with increasing work function. The tunneling barrier is maximum in case of Palladium (Fig. 5c) due to higher work function at the gate metal electrodes. Also, higher drain bias attracts more n-type charges near the drain area. The collective effect is reflected as a delayed peak in the electric field graph as seen in Fig. 2a. The primary reason in energy band shifts is the higher work function that incites a higher concentration of p-type carriers. Moreover, on account of high-level work function of 5.93 eV applied at the source, p + pockets induced facilitate the increased tunneling near source-channel interface than near the drain region. This results in an expanded bandgap near the drain region in contrast to source-channel space, as is visible in the graphs.

4 Results and discussion

JL-VTFET is used as a transducer here. WFV owing to gas molecules' reactions with the catalytic metal surface is reflected in a commensurable electrical signal, i.e., a modification in I_{ds}. Figure 6a–c represent the effect of variation of 50 meV, 100 meV, 150 meV and 200 meV in work function on the drain current (I_{ds}) for Cobalt, Molybdenum and Palladium respectively. From the graphs, insinuations can be drawn regarding exponential decrement in I_{doff} as compared to I_{don}. A change of the order of mV in the work function has greater impact on I_{doff}, providing much higher sensitivity in the subthreshold regime [8]. The band-to-band (BTBT) tunneling is confined strictly within the lean channel and source boundaries [11]. This contributes to variations in work function and since TFETs are less immune to work function variations of metal electrodes, this brings a change in V_{th}. This contributes to exponential changes in I_{doff}. Thus, sensitivity in terms of I_{doff} (S_{Idoff}) can be reviewed for low power applications.

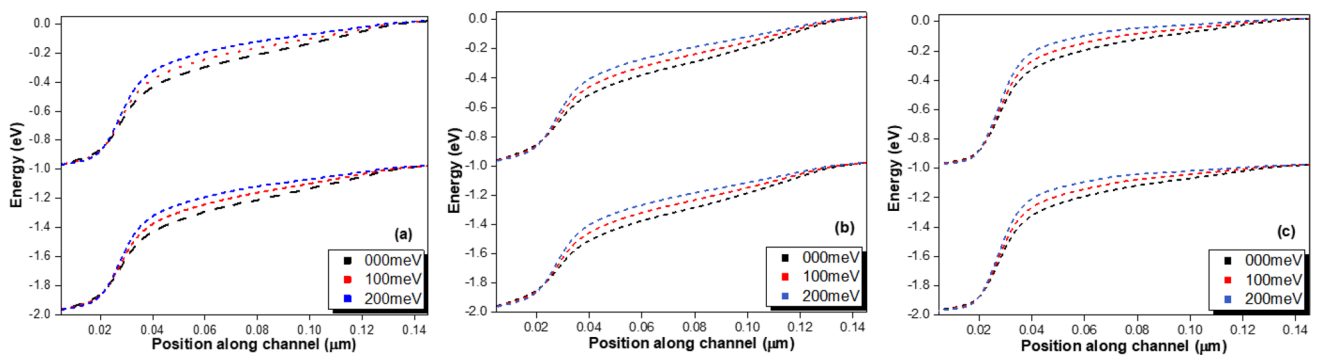Equation (5) represents the sensitivity equation used for the proposed device [8].

Fig. 5 Energy band diagram (valence band and conduction band) for **a** Cobalt, **b** Molybdenum, and **c** Palladium w.r.t work function variations of 100 meV and 200 meV
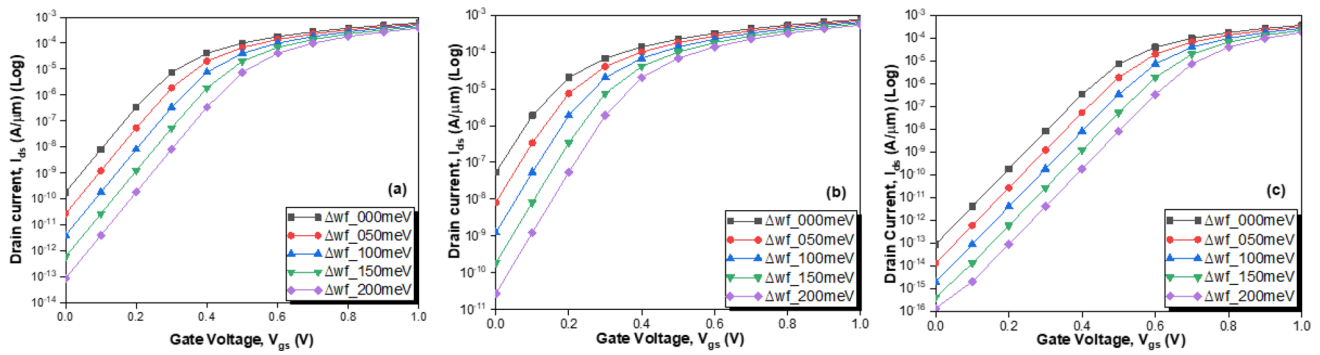
Fig. 6 Drain current graphs with and without gas molecules for JL-VTFET for **a** Cobalt, **b** Molybdenum, and **c** Palladium

$$S_{\text{Idoff}} = \frac{I_{\text{doff(before gas adsorption)}}}{I_{\text{doff(after gas adsorption)}}} \tag{5}$$

The sensitivity factors for JL-VTFET based sensor using Cobalt, Molybdenum, and Palladium as the gate metal electrodes are enlisted in Tables 2, 3, 4, respectively.

With increase in work function, the steepness of the energy band diagram of source-channel interface decreases leading to a reduction in tunneling probability to the conduction band. The duality of a high enough potential barrier is in the prevention of tunneled electrons from overcoming it, or, allowing only those with adequate energy to flow towards the drain directly from the channel [7]. Thus, only those electrons having high enough energy become part of BTBT mechanism. This causes the exponential decrement in I_{doff} with increasing WFV. The ON state current (I_{don}) is not much influenced by the work function variations. Figure 7a reveals that the ON/OFF ratio value ($I_{\text{don}}/I_{\text{doff}}$) is noticeably large for Palladium, preceded by

Cobalt and then Molybdenum, owing to their work functions' values.

Figure 7b shows the I_{doff} sensitivity curves for various metals used as gate electrodes. S_{Idoff} calculation is done based on Eq. (5). OFF current sensitivity is considerably higher for lower work function metals, i.e., Molybdenum and Cobalt ($\sim 1.99 \times 10^3$ and 2.09×10^3), as compared to Palladium ($\sim 6.43 \times 10^2$), due to less influence of higher work function variations and thus lesser potential barrier effects. As OFF current decreases, the sensitivity value increases, as is visible from the graph.

5 Conclusion

The notion of single metal gate junctionless VTFET as a highly sensitive gas detector has been implemented in this literature. Highly reactive catalytic metal Palladium gives high sensitivity of 6.43×10^3 for Ammonia detection while Molybdenum and Cobalt gate metals yield a sensitivity in
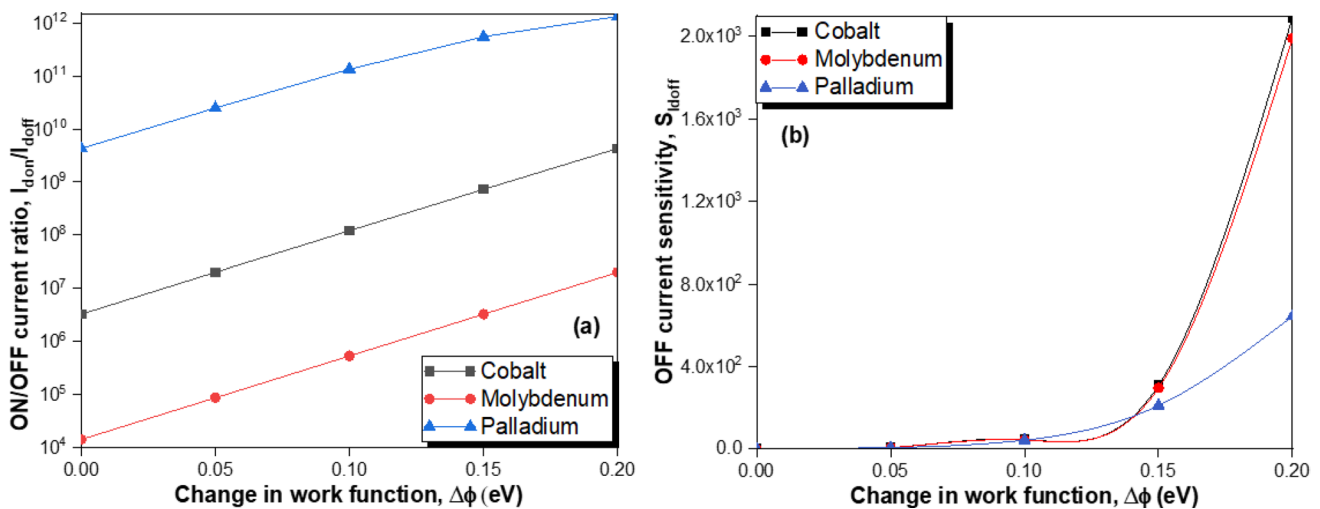

Fig. 7 **a** $I_{\text{don}}/I_{\text{doff}}$ current ratio **b** OFF current sensitivity of JL-VTFET sensor for Palladium, Molybdenum and Cobalt

the range of 1.99×10^3 and 2.09×10^3, for a minimalitic change of 200 meV in work function, thus proving the effectiveness of the proposed structure. The I_{don}/I_{doff} ratios achieved showcase the proposed structure as an efficient choice. Further optimization may be done in terms of gate engineering and channel related parameters. To implement a cost effective, low power gas sensor with the less on-chip area, studying the device behavior in the subthreshold regime provides scope for enhanced sensitivity. The vertical architecture, with increased gate controllability and the absence of sharp doping gradient makes JL-VTFET a promising candidate for future research on gas sensing devices.

References

1. N. Jayaswal, A. Raman, N. Kumar, S. Singh, Design and analysis of electrostatic-charge plasma based dopingless IGZO vertical nanowire FET for ammonia gas sensing. Superlattices Microstruct. **125**, 256–270 (2019)
2. I. Lundstrom, M. Armgarth, A. Spetz, F. Winquist, Gas sensors based on catalytic metal-gate field-effect devices. Sens. Actuators **10**, 399–421 (1986)
3. K. Tsukada, M. Kariya, T. Yamaguchi, T. Kiwa, H. Yamada, T. Maehara, T. Yamamoto, S. Kunitsugu, Dual gate field effect transistor hydrogen gas sensor with thermal compensation. Jpn. J. Appl. Phys. **49**, 024206-1-024206–5 (2010)
4. K. Scharnagl, A. Karthigeyan, M. Burgmair, M. Zimmer, T. Doll, I. Eisele, Low temperature hydrogen detection at high concentrations: comparison of platinum and iridium. Sens. Actuators B **80**, 163–168 (2001)
5. A. Gnudi, S. Reggiani, E. Gnani, G. Baccarani, Analysis of threshold voltage variability due to random dopant fluctuations in junctionless FETs. IEEE Electron Device Lett. **33**(3), 336–338 (2012). https://doi.org/10.1109/LED.2011.2181153
6. W. Li, J. Woo, Vertical P-TFET with a P-Type SiGe Pocket. IEEE Trans. Electron Devices **67**(4), 1480–1484 (2020)
7. E. Ko, H. Lee, J. Park, C. Shin, Vertical tunnel FET: design optimization with triple metal-gate layers. IEEE Trans. Electron Devices **63**(12), 5030–5035 (2016). https://doi.org/10.1109/TED.2016.2619372
8. R. Gautam, M. Saxena, R.S. Gupta, M. Gupta, Gate-all-around nanowire MOSFET with catalytic metal gate for gas sensing applications. IEEE Trans. Nanotechnol. **12**(6), 939–944 (2013). https://doi.org/10.1109/TNANO.2013.2276394
9. B. Lee, J. Oh, H. Tseng, R. Jammy, H. Huff, Gate stack technology for nanoscale devices. Mater. Today **9**, 32–40 (2006). https://doi.org/10.1016/S1369-7021(06)71541-3
10. D. K. Dash, P. Saha, A. Mahajan and S. K. Sarkar, *3-D analytical modeling of dual-metal front-gate stack tri-gate SON-TFET with graded channel engineering.* 2017 IEEE Calcutta Conference (CALCON) (Kolkata, 2017), pp. 199–204, https://doi.org/10.1109/CALCON.2017.8280724
11. K.M. Choi, W.Y. Choi, Work-function variation effects of tunneling field-effect transistors (TFETs). IEEE Electron Device Lett. **34**(8), 942–944 (2013). https://doi.org/10.1109/LED.2013.2264824
12. F. Chen, H. Ilatikhameneh, Y. Tan, G. Klimeck, R. Rahman, Switching mechanism and the scalability of vertical-TFETs. IEEE Trans. Electron Devices **65**(7), 3065–3068 (2018). https://doi.org/10.1109/TED.2018.2831688
13. S. Badgujjar, G. Wadhwa, S. Singh et al., Design and analysis of dual source vertical tunnel field effect transistor for high performance. Trans. Electr. Electron. Mater. **21**, 74–82 (2020). https://doi.org/10.1007/s42341-019-00154-2
14. ATLAS Device Simulation Software (Silvaco Int., Santa Clara 2016)
15. K. Nigam, P. Kondekar, D. Sharma, High frequency performance of dual metal gate vertical tunnel field effect transistor based on work function engineering. Micro Nano Lett. **11**(6), 319–322 (2016)
16. G. Wadhwa, B. Raj, Label free detection of biomolecules using charge-plasma-based gate underlap dielectric modulated junctionless TFET. J. Electron. Mater. **47**, 4683–4693 (2018). https://doi.org/10.1007/s11664-018-6343-1
17. N. Seema, C. Sudakar Singh, Performance investigation of electrode work-function engineered hetero-dielectric buried oxide vertical TFET. IET Circuits, Devices & Systems. **13**(7), 1027–1031 (2019). https://doi.org/10.1049/iet-cds.2018.5111IET Digital Library, https://digital-library.theiet.org/content/journals/10.1049/iet-cds.2018.5111
18. K.S. Singh, S. Kumar, K. Nigam, V.A. Tikkiwal, Tunnel field effect transistor for ultra low power applications: a review. In *2019 International Conference on Signal Processing and Communication (ICSC)* (IEEE, 2019), pp. 286–291. https://doi.org/10.1109/ICSC45622.2019.8938260
19. R.N. Goswami, S. Poorvasha, B. Lakshmi, Tunable work function in Junctionless Tunnel FETs for performance enhancement. Aust. J. Electr. Electron. Eng. **15**(3), 80–85 (2018). https://doi.org/10.1080/1448837X.2018.1525173
20. Ajay, R. Narang, M. Saxena, M. Gupta, Modeling and simulation investigation of sensitivity of symmetric split gate junctionless FET for biosensing application. IEEE Sens. J. **17**(15), 4853–4861 (2017). https://doi.org/10.1109/JSEN.2017.2716102
21. Y. Dan, S. Evoy, A.T. Johnson, Chemical gas sensors based on nanowires. arXiv preprint arXiv:0804.4828 (2008)
22. G.F. Fine, L.M. Cavanagh, A. Afonja, R. Binions, Metal oxide semi-conductor gas sensors in environmental monitoring. Sensors **10**(6), 5469–5502 (2010)
23. J. Wöllenstein, M. Burgmair, G. Plescher, T. Sulima, J. Hildenbrand, H. Böttner, I. Eisele, Cobalt oxide based gas sensors on silicon substrate for operation at low temperatures. Sens. Actuators B Chem. **93**(1–3), 442–448 (2003)
24. D. López-Torres et al., Sensitivity optimization of a microstructured optical fiber ammonia gas sensor by means of tuning the thickness of a metal oxide nano-coating. IEEE Sens. J. **19**(13), 4982–4991 (2019). https://doi.org/10.1109/JSEN.2019.2901361
25. B. Timmer, W. Olthuis, A. Van Den Berg, Ammonia sensors and their applications—a review. Sens. Actuators B Chem. **107**(2), 666–677 (2005)